Amino Acids (2011) 41:351–361
DOI 10.1007/s00726-010-0575-6

ORIGINAL ARTICLE

Quantitative proteome analysis of the 20S proteasome of apoptotic Jurkat T cells

Frank Schmidt · Burkhardt Dahlmann · Hanne K. Hustoft · Christian J. Koehler · Margarita Strozynski · Alexander Kloß · Ursula Zimny-Arndt · Peter R. Jungblut · Bernd Thiede

Received: 1 December 2009 / Accepted: 17 March 2010 / Published online: 3 April 2010

Abstract Regulated proteolysis plays important roles in cell biology and pathological conditions. A crosstalk exists between apoptosis and the ubiquitin–proteasome system, two pathways responsible for regulated proteolysis executed by different proteases. To investigate whether the apoptotic process also affects the 20S proteasome, we performed three independent SILAC-based quantitative proteome approaches: 1-DE/MALDI-MS, small 2-DE/MALDI-MS and large 2-DE/nano-LC–ESI–MS. Taking the results of all experiments together, no quantitative changes were observed for the α- and β-subunits of the 20S proteasome except for subunit α7. This protein was identified in two protein spots with a down-regulation of the more acidic protein species (α7a) and up-regulation of the more basic protein species (α7b) during apoptosis. The difference in these two α7 protein species could be attributed to oxidation of cysteine-41 to cysteine sulfonic acid and phosphorylation at serine-250 near the C terminus in α7a, whereas these modifications were missing in α7b. These results pointed to the biological significance of posttranslational modifications of proteasome subunit α7 after induction of apoptosis.

Keywords Apoptosis · 5-Fluorouracil · 20S proteasome · Phosphorylation · SILAC

Abbreviations

19S-Reg	19S regulator complex
5-FU	5-Fluorouracil
H/L	Heavy to light
PARP1	Poly (ADP-ribose) polymerase-1
SILAC	Stable isotope labeling with amino acids in cell culture

Introduction

Many important intracellular processes are regulated by transcription, translation and protein degradation. In eukaryotic cells, the ubiquitin–proteasome pathway is the major non-lysosomal pathway for protein degradation. This proteolytic pathway is based on the coordinated and synergistic activity of two enzymatic systems: proteins are initially targeted for proteolysis by the attachment of a polyubiquitin chain catalyzed by the ubiquitin-conjugating system and are then recognized and rapidly degraded to small peptides by the proteasome (Hershko and

This article is published as part of the Special Issue on Protein Species and Time Schedule.

Electronic supplementary material The online version of this article (doi:10.1007/s00726-010-0575-6) contains supplementary material, which is available to authorized users.

F. Schmidt · H. K. Hustoft · C. J. Koehler · M. Strozynski · B. Thiede (✉)
The Biotechnology Centre of Oslo, University of Oslo, Gaustadalleen 21, Blindern, P.O. Box 1125, 0317 Oslo, Norway
e-mail: bernd.thiede@biotek.uio.no

F. Schmidt
Interfaculty Institute for Genetics and Functional Genomics, University of Greifswald, Greifswald, Germany

B. Dahlmann · A. Kloß
Institute of Biochemistry, Charité-Universitätsmedizin, Berlin, Germany

U. Zimny-Arndt · P. R. Jungblut
Max Planck Institute for Infection Biology, Core Facility Protein Analysis, Berlin, Germany

Ciechanover 1998; Glickman and Ciechanover 2002). The proteasome is a macromolecular complex composed of a cylindrical 20S core particle (20S proteasome), which is capped by one or two 19S regulator complexes (19S-Reg) (Dahlmann 2005). In mammalian cells, three additional activators are known (PA28 $\alpha\beta$, PA28γ, and PA200), which may bind to a 20S proteasome or to a 19S Reg-20S proteasome complex and thus form various proteasome-activator complexes (Rechsteiner and Hill 2005). The 20S proteasome is built of four stacked seven-membered rings that are composed of seven different α-subunits and seven different β-subunits yielding a stoichiometry: α1-7, β1-7, β1-7, α1-7 (Bochtler et al. 1999). The alpha subunits bind the various regulator and activator complexes, while three of the beta subunits (β1, β2, β5) catalyze the peptide bond hydrolysis. A mechanism to modify the proteolytic properties of proteasomes is the replacement of the three active site-containing β-subunits by the so-called immunosubunits, β1i, β2i and β5i, the synthesis of which is induced by interferon-γ (Tanaka et al. 1997). Thus, besides some intermediate forms of 20S proteasomes (Dahlmann et al. 2000; Drews et al. 2007; Raijmakers et al. 2008), two major subpopulations exist, immunoproteasomes and standard proteasomes (constitutive or housekeeping proteasomes).

The inhibition of protein degradation through the ubiquitin–proteasome pathway is a recently developed approach for cancer treatment. Most importantly, Bortezomib was the first proteasome inhibitor approved for treating multiple myeloma and mantle cell lymphoma. The specific antitumor effect of proteasome inhibitors relies mainly on the activation of apoptosis, the major form of programmed cell death that occurs in multicellular organisms (Orlowski and Kuhn 2008). Several studies have shown that the ubiquitin–proteasome pathway mediates the degradation of apoptotic regulators, including proapototic (e.g., Bax, Bak, Bid, Bik, p53, caspases and Smac/DIABLO) and antiapoptotic (e.g., Mcl-1, XIAP, cIAP1 and cIAP2) proteins (Liu et al. 2007). On the other hand, it has also been suggested that proteasome function may be inhibited during apoptosis. Interestingly, the caspase-dependent cleavage of three specific subunits (Rpn2, Rpn10 and Rpt5) of the 19S regulator complex of human proteasomes during apoptosis inhibited the proteasomal degradation of the substrates and supported the apoptotic program (Sun et al. 2004; Adrain et al. 2004).

Several proteomics approaches have been applied to study the proteasome. Mostly, 2-DE gels and stable isotope tagging were applied to quantify the proteasomal subunits and its species (Schmidt et al. 2006; Dahlmann et al. 2000; Kuckelkorn et al. 2002; Claverol et al. 2002; Iwafune et al. 2004; Froment et al. 2005). The interacting network of the yeast 26S proteasome was analyzed combining in vivo cross-linking, tandem affinity purification and stable isotope labeling with amino acids in cell culture (SILAC) revealing 42 novel interaction partners (Guerrero et al. 2006). It has become clear that protein speciation (Jungblut et al. 2008) can also be observed in proteasomes (Uttenweiler-Joseph et al. 2008; Huang and Burlingame 2005). Most of the subunits occur with at least two spots on 2-DE gels. Glycosylated (Zong et al. 2008), phosphorylated (Iwafune et al. 2004), acetylated (Schmidt et al. 2006; Kimura et al. 2000) and oxidized (Zong et al. 2008) protein species were identified.

In the present study, stable isotope labeling with amino acids in cell culture (SILAC) (Ong et al. 2002) was applied to compare the 20S proteasome of apoptotic with those of non-apoptotic Jurkat T cells quantitatively. Apoptosis was induced with 5-fluorouracil (5-FU), a well-known anticancer drug that induces DNA damage and subsequently apoptosis. Two protein species of proteasomal subunit α7 were found with opposing quantitative changes during apoptosis, whereas all other proteasomal subunits seemed to be unchanged. Detailed mass spectrometric analysis revealed that the two protein species of proteasomal subunit α7 differed in posttranslational modifications.

Materials and methods

Cell culture, SILAC and induction of apoptosis

The Jurkat T cell line E6 was grown in RPMI-1640 (Invitrogen, Oslo, Norway) without arginine and lysine supplemented with 5% fetal calf serum (Invitrogen, Oslo, Norway), 0.2 M dialyzed glutamine, 100 U/ml penicillin, 50 mg/l arginine-$^{12}C_6$ and 100 mg/l lysine-$^{12}C_6$ (light) or 50 mg/l arginine-$^{13}C_6$ monohydrochloride and 100 mg/l lysine-$^{13}C_6$ (heavy) (Sigma–Aldrich, Oslo Norway) at 37°C in a 5% CO_2 environment. The cells were split four times and the incorporation of the amino acids was checked using acidic extraction of peptides from the cells and MALDI-MS analysis (Schmidt et al. 2007). For chemotherapeutic drug treatment, Jurkat T cells were exposed to 400 µM 5-FU (Sigma–Aldrich, Oslo, Norway) for 0 and 32 h before harvesting. Cell pellets were resuspended in lysis buffer (25 mM Tris–HCl, 50 mM KCl, 3 mM EDTA, 1% Triton X-100, 5 mM β-mercaptoethanol, pH 7.1) supplemented with protease (3 mM benzamidine, 10 µM leupeptin and 1 mM PMSF) and phosphatase inhibitors (30 mM NaF, 1 mM Na_3VO_4, 20 mM $Na_4P_2O_7$) and homogenized using a pestle pellet. Cleavage of poly (ADP-ribose) polymerase-1 (PARP1) by caspase-3 is a marker of apoptosis and was analyzed using immunoblotting with PARP-1 antibody (1:1,000) (Cell Signaling, Beverly, MS, USA). Protein samples were separated by SDS-PAGE and

transferred onto PVDF membranes (Immobilon P, Millipore, Oslo, Norway) using a Mini Trans-Blot cell (Bio-Rad, Munich, Germany). HRP-conjugated anti-mouse- or anti-rabbit IgG (1:10,000) were used as secondary antibodies. Membranes were developed by SuperSignal West Pico Chemiluminescent (VWR, Oslo, Norway).

Enrichment of the 20S proteasome

Total extracts from lysed cells (2.5×10^7) were separated by gel filtration using an FPLC system with a Superose 6 column (analytical grade, 300 × 10 mm) using 20 mM Tris–HCl buffer, pH 7.5, containing 1 mM EDTA, 1 mM NaN_3 and 1 mM DTT (TEAD buffer). Detection of the 20S proteasome-containing fractions was performed with fluorogenic substrate Suc-Leu-Leu-Val-Tyr-MCA to measure the chymotrypsin-like activity as previously described (Dahlmann et al. 2000). Pooled 20S proteasome enriched fractions were further separated by strong anion exchange chromatography (MiniQ column) in a SMART system. The 20S proteasome was eluted by means of an increasing gradient of 0–500 mM NaCl in TEAD buffer. All chromatographic systems and columns were purchased from GE-Healthcare, Freiburg, Germany. Three independent preparations derived from SILAC-labeled controls and apoptotic Jurkat T cells were made for the subsequent analyses.

SDS-PAGE

SDS-PAGE was performed applying 16 µg proteasomal subunits on top of a 12-cm long 4% stacking gel and 10% separation gel using a Multigel-long gel system (BioSite, Täby, Sweden) (Laemmli 1970). Gels were stained with Coomassie Brilliant Blue G-250 (Serva, Heidelberg, Germany) employing the blue silver staining technique with slight modifications (Candiano et al. 2004). Fixation was performed with 50% ethanol/2% phosphoric acid for 1 h, incubation with 34% ethanol/2% phosphoric acid/17% ammonium sulfate for 1 h, and staining with 20% methanol/10% phosphoric acid/10% ammonium sulfate for 1 h. Finally, the gels were washed once for 30 min with 25% ethanol and three times with water.

Two-dimensional gel electrophoresis

The dried proteasomal proteins were dissolved in 9 M urea, 70 mM DTT, 2% carrier ampholytes Servalyte 2–4 (Serva, Heidelberg, Germany) and protease inhibitors (TLCK, leupeptin, E64, pepstatin A; 25 µM). The carrier ampholyte isoelectric focusing method was combined with SDS polyacrylamide gel electrophoresis in a small gel (7 cm × 8 cm) (Jungblut and Seifert 1990) or a large gel (23 cm × 30 cm) technique (Zimny-Arndt et al. 2009). Proteasomal subunits (5 µg) were applied to the small gel and 40 µg to the large one. Proteins were stained with Coomassie Brilliant Blue G-250 (Doherty et al. 1998).

MALDI-TOF/TOF–MS

Coomassie G-250-stained SDS-PAGE bands or 2DE gel spots were excised with a scalpel for in-gel digestion with 0.1 µg of trypsin in 20 µl of 50 mM ammonium bicarbonate, pH 7.8 (Thiede et al. 2005). An Ultraflex II (Bruker Daltonics, Bremen, Germany) MALDI-TOF/TOF mass spectrometer was used after external calibration. Instrument parameters were set according to previously described methods (Schmidt et al. 2009). The samples were analyzed in the TOF mode for generation of peptide mass fingerprints (PMF), mixed with matrix [20 mg/ml α-cyano-4-hydroxycinnamic acid in 0.3% aqueous trifluoroacetic acid/acetonitrile (2:1)] and applied to a stainless steel sample holder. MS spectra were transformed into peak lists by using the software FlexAnalysis version 2.4. (Bruker Daltonics, Bremen, Germany). The peak areas of the peak pairs were used to calculate the relative ratios (H/L) of the proteins.

Nano-LC–LTQ-Orbitrap-MS

The stained 2-DE spots were excised for in-gel digestion with 0.1 µg of trypsin (Promega, Madison, WI, USA) in 20 µl of 25 mM ammonium bicarbonate, pH 7.8 at 37°C for 16 h, and further prepared for mass spectrometry. The separation of peptides was performed using a Dionex Ultimate 3000 nano-LC system (Sunnyvale CA, USA) connected to a linear quadrupole ion trap-Orbitrap (LTQ-Orbitrap) mass spectrometer (ThermoElectron, Bremen, Germany) equipped with a nano-ESI source. For liquid chromatography separation, we used an Acclaim PepMap 100 column (C18, 3 µm, 100 Å) (Dionex, Sunnyvale CA, USA) capillary of 12-cm bed length. The flow rate used was 300 nL/min for the nano column, and the solvent gradient used was 7% B to 50% B in 20 min. Solvent A was 0.1% formic acid, whereas aqueous 90% acetonitrile in 0.1% formic acid was used as solvent B. The mass spectrometer was operated in the data-dependent mode to automatically switch between Orbitrap-MS and LTQ-MS/MS acquisition. Survey full scan MS spectra from *m/z* 300 to 2,000 were acquired in the Orbitrap with resolution $R = 60.000$ at *m/z* 400 after accumulation to a target of 1,000,000 charges in the LTQ. The method used allowed sequential isolation of the most intense ions, up to six, depending on signal intensity, for fragmentation on the linear ion trap using collision-induced dissociation (CID)

at a target value of 100,000 counts. For accurate mass measurements, the lock mass option was enabled in MS mode and the polydimethylcyclosiloxane (PCM) ions generated in the electrospray process from ambient air were used for internal recalibration during the analysis (Olsen et al. 2005). Target ions already selected for MS/MS were dynamically excluded for 60 s. Other instrument parameters have been previously described (Koehler et al. 2009).

Raw data were processed using Thermo Proteome Discoverer software (v. 1.0 build 43) to generate Mascot generic files (*.mgf) and a database search by tandem mass spectrometry ion search algorithms from the Mascot in-house server (v2.2.1) by database comparisons (Perkins et al. 1999) against the human entries from the SwissProt (12.12.2008, 20,411 sequences). A mass tolerance of 10 ppm for the precursor and 0.5 Da for MS/MS fragments were applied. Furthermore, trypsin was selected as enzyme considering up to one missed cleavage site, peptide charge 2+ and 3+, and variable protein modifications were allowed such as oxidation (M), *N*-acetyl (protein), propionamide (C), pyro-glu (N-term Q) and $^{13}C_6$ of arginines and lysines. Significant threshold was set to $p < 0.05$, and MudPIT scoring was applied with an ion score cutoff of 20. For automatic error-tolerant searches of uninterpreted MS/MS data, the same parameters were used with the exception that only oxidation (M) and *N*-acetyl (protein) were allowed (Creasy and Cottrell 2002). Posttranslational modifications were assigned by Mascot and manually evaluated.

Relative quantification ratios of identified proteins were derived by the open source software MSQuant v 1.4.3b4 (msquant.sourceforge.net). Peptide ratios were obtained by calculating the extracted ion chromatograms (XICs) of the monoisotopic peaks of light and heavy forms of peptides. The total XIC for each of the peptide forms was obtained by summing the XIC in consecutive MS cycles for the duration of their respective LC–MS peaks in the total ion chromatogram using Orbitrap-MS scans. The total XICs were used to calculate the relative peptide ratios of the same protein and the respective standard deviation. In addition, peptide ratios obtained by using the MSQuant software were inspected manually. The Grubbs' test for outliers was applied to determine which protein spots were significantly regulated with less than 5% probability to belong to the unregulated population of ratios (Grubbs 1969).

Results

The analysis of the 20S proteasome was performed with Jurkat T cells using SILAC to compare quantitatively the light (L) labeled control with the heavy (H) labeled apoptotic state. Apoptosis was induced using 400 µM 5-FU, and the appearance of apoptosis was verified after 32 h using immunoblotting of PARP-1, which showed the well-known caspase cleavage product at 89 kDa (Fig. 1a). The proteolytic activities of proteasomes, as measured by the use of the substrates Suc-Leu-Leu-Val-Tyr-MCA (chymotrypsin-like activity), Bz-Val-Gly-Arg-MCA (trypsin-like activity) and Z-Leu-Leu-Glu-MCA (caspase-like activity), were not different within cell extracts of apoptotic and non-apoptotic cells (data not shown). The 20S proteasome was enriched using gel filtration, whereby the fractions containing the 20S proteasome (fractions 24–28) were detected by measuring the chymotrypsin-like activity with the fluorogenic substrate Suc-Leu-Leu-Val-Tyr-MCA (Fig. 1b). Subsequently, the proteasome was further purified by strong anion exchange chromatography on a Mini Q column (Fig. 1c).

Apoptosis-mediated quantitative changes of the 20S proteasome detected by 1-DE/MALDI-MS

The analysis of the 20S proteasome-containing fractions after gel filtration and strong anion exchange chromatography using SDS-PAGE revealed several bands in the mass region of the proteasomal subunits between 20 and 30 kDa (Fig. 1b). This mass region was sliced into 30 bands to detect minimal changes in M*r* and each of them was analyzed after digestion with trypsin using MALDI-MS. All seven α-subunits and five of the seven *β*-subunits were detected with SILAC peak pairs by MALDI-MS (Table 1). The heavy-to-light (H/L) ratios of these proteins were determined to be between 0.95 and 1.16 with the exception of proteasomal subunit α7 (also known as PSMA3 and C8), which was significantly regulated in one gel slice with an H/L ratio of 0.64 (Table 1). Notably, proteasomal subunit α7 was identified in another gel slice with a noticeable different H/L value of 1.06 (Table 1).

Apoptosis-mediated quantitative changes of the 20S proteasome detected by small 2-DE/MALDI-MS

To confirm the deviant H/L ratios of proteasomal subunit α7 in comparison to the other proteasomal subunits and to increase the sequence coverage, we performed small 2-DE gel electrophoresis for improved separation of the proteins (Fig. 2). All α- and *β*-subunits were identified as well as two immunosubunits (*β*1i and *β*5i). All protein species besides proteasomal subunit α7 revealed an H/L ratio between 0.91 and 1.09 (Table 1). By contrast, the two species of proteasomal subunit α7 displayed the lowest

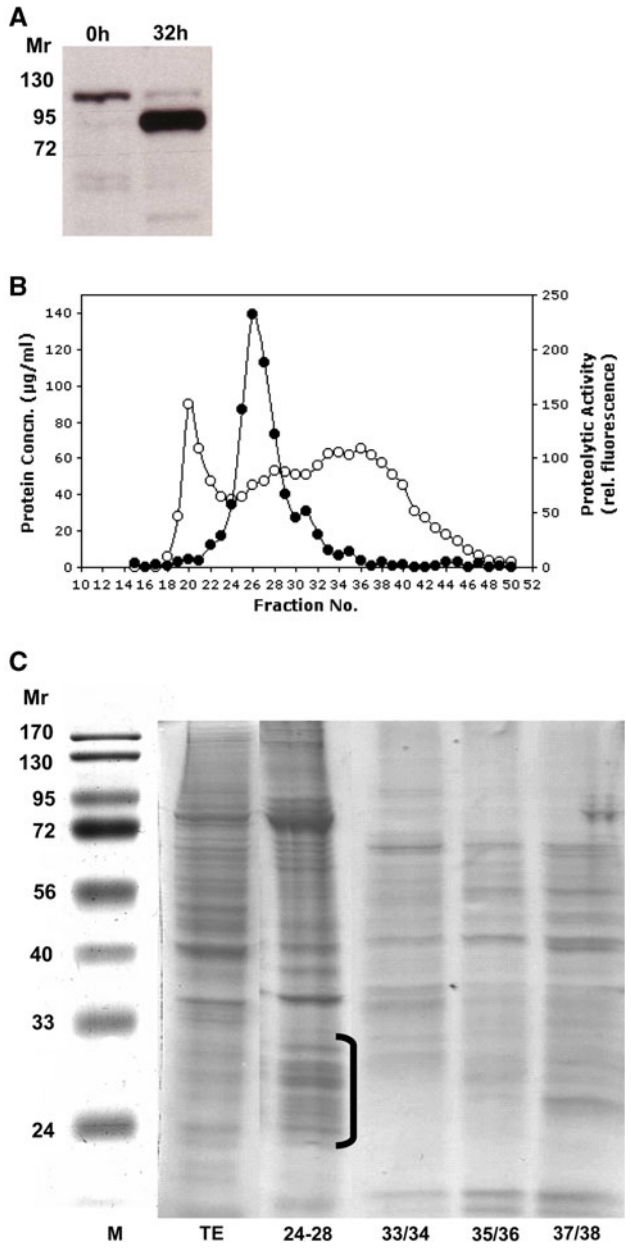

Fig. 1 Cleavage of PARP-1 during 5-FU-induced apoptosis and purification of the 20S proteasome. Poly [ADP-ribose] polymerase 1 (PARP-1) is a substrate of caspase-3 and the cleavage of this protein is a hallmark of apoptosis. The expected mass shift of the full-length protein with a molecular mass of 114 kDa to the C-terminal cleavage product with 89 kDa was observed at 32 h of incubation with 5-FU (**a**). A total Jurkat T cell lysate was subjected to gel filtration on Superose 6 and protein concentrations measured by means of Bradford assay (*open circles*) (**b**). The 20S proteasome-containing fractions were detected by measuring the chymotrypsin-like activity using the fluorogenic substrate Suc-Leu-Leu-Val-Tyr-MCA (*filled circles*). The proteasome-containing fractions were pooled and analyzed by SDS-PAGE (**c**). The protein bands in the region of 20–30 kDa contained 20S proteasome subunits

(0.81, α7a) and the highest (1.14, α7b) H/L value (Table 1) with a sequence coverage of 46% for α7a and 50% for α7b using peptide mass fingerprinting.

Apoptosis-mediated quantitative changes of the 20S proteasome detected by large 2-DE/nano-LC–ESI–MS

To further verify the observed effect on proteasomal subunit α7, we increased even more the resolution of protein separation using large 2-DE gels (Fig. 3) in combination with peptide separation by nano-LC, which was connected online to high-resolution LTQ-Orbitrap mass spectrometry. All α-subunits, β-subunits and two immunosubunits (β1i and β5i) were identified and quantified. Again, two spots were identified as proteasomal subunit α7, both with a sequence coverage of 43% (Supplementary Table 1) and with a difference of 0.35 in H/L value, whereas the differences of all other protein spots of identical proteins were below 0.13 (Table 1).

Changes in posttranslational modifications of proteasomal subunit α7 due to apoptosis

Based on the results of three independent experiments as shown above, we searched for differences between the two protein spots of proteasomal subunit α7. Therefore, the automatic error-tolerant search function in Mascot was applied to identify posttranslational modifications using the LTQ-Orbitrap data. Thereby, a phosphorylation site at the protein N terminus $_{2}$SSIGTGYDLSASTFSPDGR$_{20}$ (Fig. 4a) with a Mascot ion score of 26 was predicted for the more basic protein spot (spot α7b in Fig. 3), whereas a phosphorylation site within the sequence $_{242}$ESLKEEDES DDDNM$_{255}$ with a Mascot ion score of 24 at the C-terminal end of the protein (Fig. 4b) was found for the more acidic spot (spot α7a in Fig. 3). Furthermore, a trioxidation of cysteine within the sequence $_{41}$CKDGVVFGVEK$_{51}$ (Fig. 4c) with a Mascot ion score of 62 was identified for the more acidic spot (spot α7a in Fig. 3), whereas the non-oxidized form of the same peptide was identified with a Mascot ion score of 46 for the more basic protein spot (spot α7b in Fig. 3). In addition, the MS and MS/MS data of these three peptides were validated manually. Actually, three SILAC-labeled peptide pairs of the peptide $_{2}$SSIGTGYDLSASTFSPDGR$_{20}$ were detected in both LC runs within the same MS scans. Considering the molecular masses and mass differences between the three peak pairs, most likely the acetylated peptide was detected as H^+ (*m/z* 980.45 and 983.46), as well as Na^+ (*m/z* 991.44 and 994.45) and K^+ (*m/z* 999.43 and 1,002.43) adducts (Fig. 5). In addition, neutral loss of the peptide with *m/z* 999.43 was not observed indicating a potassium adduct (+38 Da) of the acetylated (+42 Da) peptide, which corresponded to the same molecular mass as the phosphorylated (+80 Da) non-acetylated peptide (Fig. 4a). Furthermore, a change of the modified forms of this peptide during apoptosis was not observed considering the similar intensities (Fig. 5). However, the other two modified peptides of proteasomal

Table 1 Relative quantification of the apoptotic 20S proteasome Jurkat T cell from controls were cultured with normal $^{12}C_6$-arginine/lysine (light, L), whereas Jurkat T cells labeled with $^{13}C_6$-arginine/lysine (heavy, H) were incubated with 5-FU to induce apoptosis

Proteasomal subunit	1-DE/MALDI			2-DE/MALDI			2-DE/Orbitrap			
	H/L	(SD)	PP	H/L	(SD)	PP	H/L	(SD)	PP	Species
α1 (PSMA6)	1.00	(0.01)	4	1.01	(0.08)	5	1.00	(0.10)	40	α1
α2 (PSMA2)	1.16	(0.12)	6	1.03	(0.11)	4	0.95	(0.10)	27	α2b
							0.86	(0.06)	6	α2a
α3 (PSMA4)	1.00	(0.09)	5	1.01	(0.10)	5	0.98	(0.10)	20	α3b
				1.06	(0.20)	5	1.08	(0.09)	12	α3a
α4 (PSMA7)	1.16	(0.05)	4	1.00	(0.11)	5	1.01	(0.13)	27	α4b
	1.01	(0.06)	6	1.01	(0.08)	6	1.02	(0.08)	9	α4a
α5 (PSMA5)	0.95	(0.11)	4	0.97	(0.12)	4	0.93	(0.13)	36	α5
	1.03	(0.06)	4							
α6 (PSMA1)	1.00	(0.07)	6	1.08	(0.16)	5	1.02	(0.14)	42	α6b
				1.03	(0.12)	5	1.05	(0.10)	37	α6a
							1.16	(0.17)	19	α6c
α7 (PSMA3)	**0.64**	(0.06)	4	**0.81**	(0.09)	6	0.87	(0.08)	22	α7a
	1.06	(0.14)	12	1.14	(0.12)	6	**1.22**	(0.10)	19	α7b
β1 (PSMB6)		nd		1.01	(0.14)	7	0.96	(0.14)	10	β1
β2 (PSMB7)	0.98	(0.01)	2	0.94	(0.10)	5	0.93	(0.01)	10	β2
β3 (PSMB3)	1.03	(0.17)	4	1.08	(0.13)	6	1.00	(0.16)	22	β3a
							1.00	(0.14)	30	β3b
β4 (PSMB2)	1.05	(0.06)	4	0.93	(0.04)	3	0.90	(0.07)	15	β4b
	1.05	(0.09)	2	0.91	(0.01)	3	0.92	(0.05)	8	β4a
β5 (PSMB5)	0.99	(0.16)	7	1.03	(0.12)	6	1.01	(0.10)	22	β5
β6 (PSMB1)	1.06	(0.10)	3	1.09	(0.18)	5	1.01	(0.11)	46	β6b
	1.05	(0.18)	3	1.03	(0.07)	4	0.89	(0.04)	5	β6a
β7 (PSMB4)		nd		1.03	(0.11)	6	1.01	(0.15)	18	β7a
				0.96	(0.07)	4	0.97	(0.09)	37	β7b
β1i (PSMB9)		nd		0.95	(0.07)	8	0.94	(0.10)	12	β1i
β5i (PSMB8)		nd		0.98	(0.13)	10	0.94	(0.10)	24	β5i

The nomenclature of proteasomal subunits was used according to Baumeister et al. (1998). The heavy-to-light (H/L) ratios, standard deviations (SD) and number of peptide pairs (PP), which were obtained applying the three different proteomics approaches, are displayed. Significant regulated ratios according to the Grubbs' test are shown in *bold*. Furthermore, the nomenclature for the protein species of the proteasomal subunits (species) according to Fig. 3 is shown. More information can be found in Supplementary Table 1

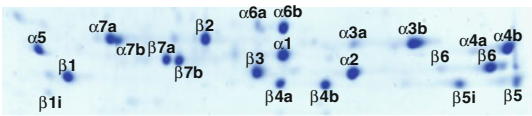

Fig. 2 Small 2-DE gel of the 20S proteasome. The enriched 20S proteasome was separated by small 2-DE gel electrophoresis and identified 20S proteasomal subunits were indicated

subunit α7a were only significantly detected in the corresponding LC run, and the phosphorylated peptide with a parent mass of *m/z* 868.30 ($z = 2+$) showed significant neutral loss at *m/z* 819.22 ($z = 2+$). Consequently, the MS data exhibited a change of phosphorylation close to the C terminus and a trioxidation of a cysteine during apoptosis.

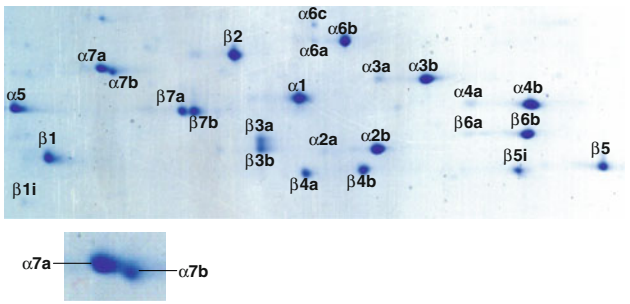

Fig. 3 Large 2-DE gel of the 20S proteasome. The enriched 20S proteasome was separated by large 2-DE gel electrophoresis. The identified 20S proteasomal subunits were indicated. The two protein spots identified as α7 were zoomed out to depict the more acidic (α7a) and the more basic (α7b) spot

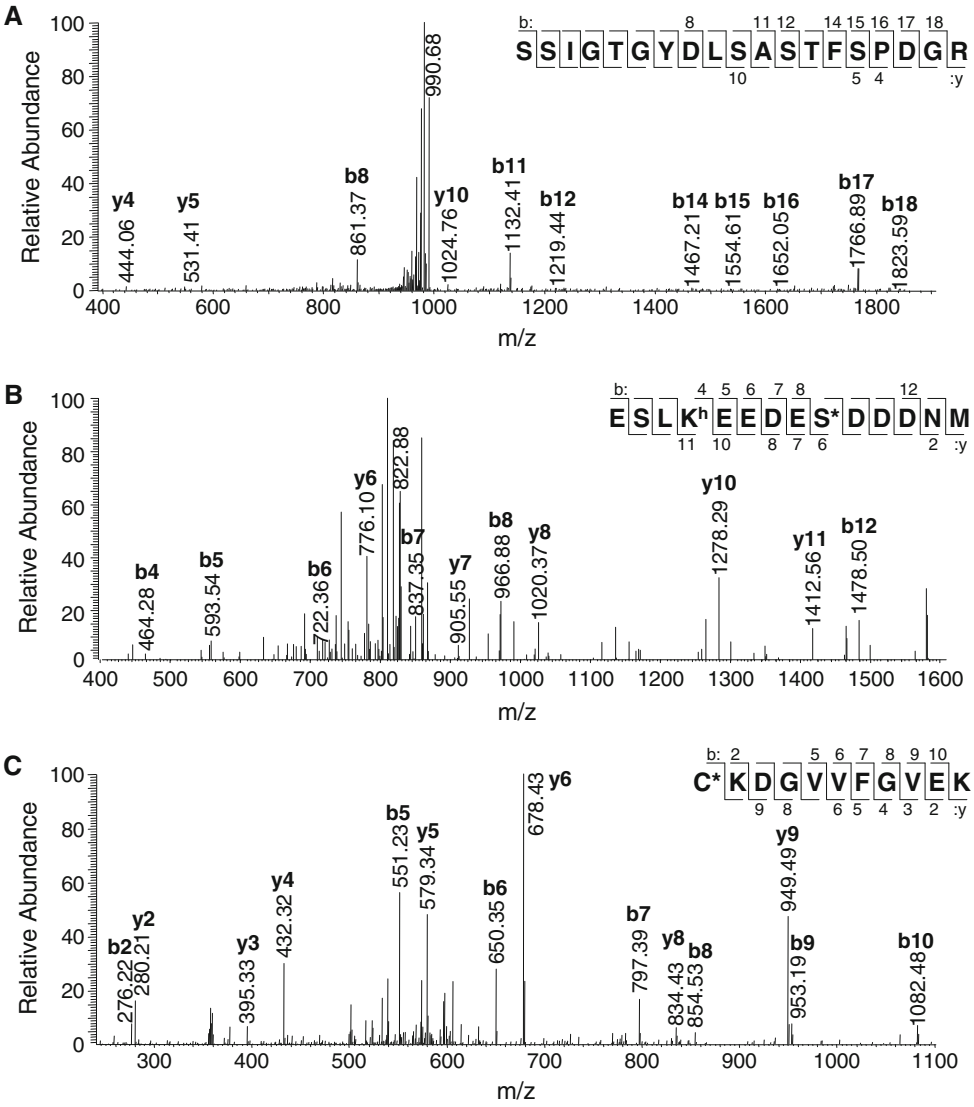

Fig. 4 MS/MS spectra of the identified modified peptides of the two different proteasomal subunit α7-species. The analysis of the two spots of α7 revealed different modifications. The peptide SSIGTGYDLSASTFSPDR (**a**) derived from the N terminus of α7 showed in the basic spot a mass difference of +80 Da in comparison to the unmodified form (Fig. 3). On the other hand, the phosphorylated peptide ESLK^{h}EEDESDDDNM (h, $^{13}C_6$-heavy form) (**b**) from the C terminus of α7 and the peptide CKDGVVFGVEK (**c**), containing a trioxidized cysteine, were only identified in the acidic spot (Fig. 3). *Asterisks* show modified amino acids

Discussion

The induction of apoptosis by various stimuli in multiple cell types results in the accumulation of ubiquitinated proteins at an early stage of apoptosis. This correlates with a decreased ability of apoptotic cells to degrade short-lived proteins through the proteasomal pathway. Interestingly, it was shown that proteasome function may be inhibited during apoptosis through targeting proteasome subunits of the 19S regulator complex for caspase-dependent cleavage. However, to our knowledge the effect of apoptosis induction on the 20S proteasome per se has not been reported yet. Therefore, we have performed a SILAC-based quantitative proteome analysis of the 20S proteasome derived from cells after induction of apoptosis with the DNA damaging agent 5-FU. Three independent proteomic approaches of three individual samples were performed and significant quantitative changes were only observed for two species of the proteasomal subunit α7. Comparing the ratios of subunit α7 spots, the more acidic α7a was down-regulated and the more basic α7b up-regulated during apoptosis. According to the nomenclature for protein species (Schluter et al. 2009), α7a has to be described as: [PSA3_HUMAN] + [AC_P25788_115] + [P_2_766] + [P_41_345] + [P_250_21], whereas α7b corresponds to [PSA3_HUMAN] + [AC_P25788_115] + [P_2_766]. Because we were not able to identify this protein species with 100% sequence coverage, this description has to be described as incomplete.

Although the main functions of α-subunits may be controlling the substrate entry pore partly by interacting with proteasome regulators such as PA28, PA200 and 19S regulator (Rabl et al. 2008), they have also been found to be able to bind various proteins, some of which are degraded in a ubiquitin-independent manner (Zhang et al. 2000; Dong et al. 2004; Alvarez-Castelao and Castano 2005). With regard to subunit α7, it was found that besides

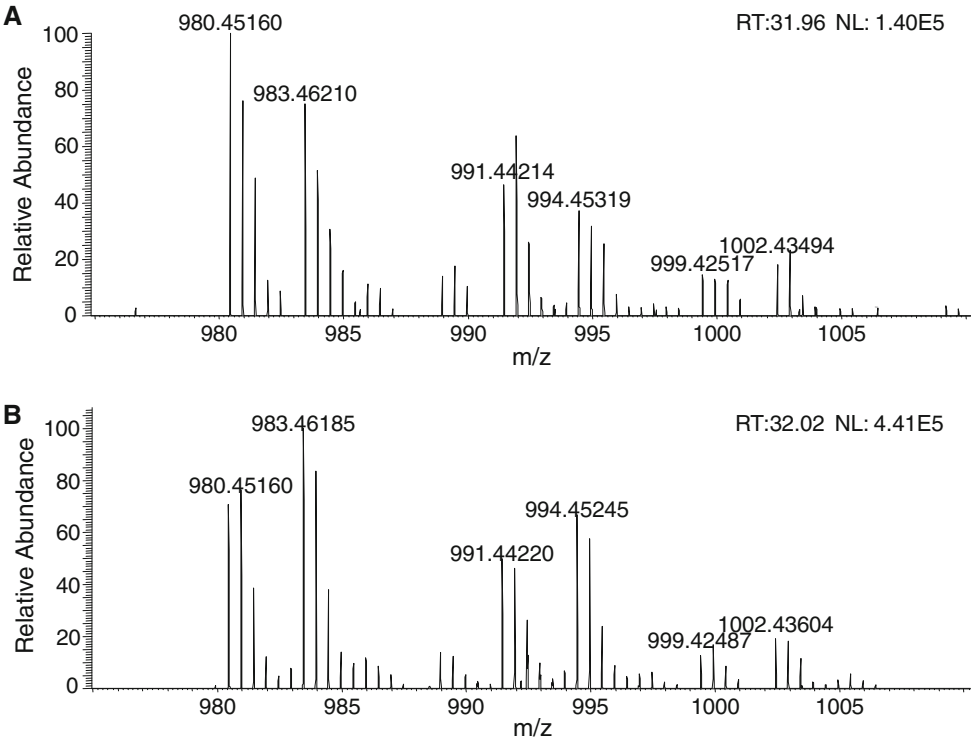

Fig. 5 MS spectra of the acetylated N-terminal tryptic peptide with different adducts derived from two different proteasomal subunit α7 spots. The MS data of the N-terminally acetylated (*m/z* 980.45 and 983.46), the sodium adduct of the acetylated (*m/z* 991.44 and 994.45) and the potassium adduct of the acetylated (*m/z* 999.45 and 1,002.43) form of SSIGTGYDLSASTFSPDR confirmed that both peptide species were down-regulated (**a**, acidic spot) or up-regulated (**b**, basic spot) during apoptosis. Notably, the mass of the potassium adduct of the acetylated peptide was identical to the phosphorylated form of the non-acetylated peptide

binding of crystalline αB (Boelens et al. 2001), it is also able to bind the cyclin-dependent kinase inhibitor p21 that can be degraded without ubiquitination (Touitou et al. 2001). During the last few years, several other subunit α7 interacting proteins have been detected, e.g., kinase aurora B (Shu et al. 2003) and Epstein–Barr virus-encoded nuclear protein EBNA3 (Touitou et al. 2001), both of which are degraded by proteasomes. The proteasome-catalyzed degradation of HBX is mediated and facilitated by binding of Id-1 to subunit α7 (Ling et al. 2008). Similarly, the steroid receptor coactivator (SRC-3) that is degraded in an ubiquitin-dependent and independent way binds to subunit α7, an interaction that can be attenuated by the atypical protein kinase C (aPKC) (Yi et al. 2008). The tumor suppressor retinoblastoma protein (Rb) can also be degraded without being ubiquitinated and binds to subunit α7, an interaction that is promoted by MDM2 (Sdek et al. 2005). MDM2 selectively binds hypophosphorylated Rb and promotes its proteasomal degradation. Similarly, MDM2 promotes the ubiquitin-independent degradation of p21 (Jin et al. 2003). Enhanced degradation of Rb and p21 can be regarded as anti-apoptotic mechanisms. Phosphorylation may affect interaction with proteasome regulator complexes or binding of substrate proteins and might well have proapoptotic consequences. This suggestion may be supported by a recent report showing that inhibitors of apoptosis (cIAP-1 and cIAP-2) are degraded by proteasomes and this degradation is regulated by a protein called ARIA (apoptosis regulator through modulating IAP expression) that interacts with proteasome subunit α7 (Ikeda et al. 2009). In accordance with our results, a change in phosphorylation of 20S proteasome subunits after induction of apoptosis by doxorubicin was also found in erythroleukemic cells (Tsimokha et al. 2007).

Our MS data indicate that a dephosphorylation of serine-250 close to the C terminus of α7 occurs during apoptosis. Phosphorylation of proteasomal subunit α7 was found by several investigators (Arrigo and Mehlen 1993; Rivett et al. 1995; Mason et al. 1996; Wehren et al. 1996). Castano et al. (1996) identified phosphorylation at serine residues 243 and 250 of the acidic C terminus. Serine phosphorylation of α7 was also detected by mass spectrometry (Wang et al. 2007; Lu et al. 2008). Phosphorylation of this subunit has no influence on the localization of proteasomes within the cell, but was found to affect the assembly of 20S proteasomes with the 19S regulator (Bose et al. 2004). Preventing the phosphorylation by serine to alanine mutation of these residues revealed reduced stability of 26S proteasomes. The negative charge of phosphoserine is needed for stable binding of the 19S regulator, since serine to aspartic acid mutation does not affect 26S proteasome stability (Bose et al. 2004). Phosphorylated serine-250 was also detected in subunit α7 of 26S proteasome from human 293 cell line (Wang et al. 2007). The state of phosphorylation of serine-243 and serine-250 seems to be controllable by γ-interferon, since treatment of cells with γ-IFN was found to reduce the level of phosphorylated α7 subunit and the level of 26S proteasomes (Bose et al. 2004).

Phosphorylation of only residue serine-250 was found in α7 subunit of 20S proteasome from human erythrocytes. This subunit was separated into three protein subunits using 2-DE: the basic protein species α7″, which was unphosphorylated; the acidic protein species, α7′, was phosphorylated; and the major spot, α7, was phosphorylated and contained an oxidized methionine residue (Claverol et al. 2002). Data obtained by immunoblot analyses were interpreted that ethanol ingestion of rats leads to hyperphosphorylation of subunit α7 of liver proteasomes in accordance with a decrease in chymotrypsin-like activity (Bardag-Gorce et al. 2004). In the C-terminal end of yeast proteasome α7 subunit three phosphoserine residues were identified; however, their state of phosphorylation did not influence the proteolytic activity of the enzyme (Iwafune et al. 2004). In vitro phosphorylation of subunit α7 was found to be catalyzed by casein kinase II (CKII) (Castano et al. 1996; Iwafune et al. 2004), a reaction strictly dependent on polylysine in yeast (Pardo et al. 1998). Interestingly, casein kinase II co-purifies with 20S proteasomes when isolated from human erythrocytes (Ludemann et al. 1993). Since especially under conditions of DNA damage CKII associates with other kinases to a multisubunit kinase complex (FACT) leading to changes in substrate specificity (Keller et al. 2001), it was hypothesized that this may also affect the phosphorylation state of proteasome subunit α7 under conditions of DNA damage and apoptosis and may thus lead to dissociation of the 26S proteasome (Mittenberg et al. 2008). In this manner, subunits of the released 19S regulator complex could interfere in the regulation of transcription (Mittenberg et al. 2008). On the other hand, a thus increased amount of 'free' 20S proteasome may have the possibility to degrade unfolded proteins (Orlowski and Wilk 2003).

Cysteine thiol modifications were increasingly recognized to occur under both physiological and pathophysiological conditions (Ying et al. 2007). Trioxidation of cysteines to cysteine sulfonic acid (or cysteic acid) is an irreversible modification and was found for e.g., in peroxiredoxins for enhanced chaperone activity (Lim et al. 2008) and in copper–zinc superoxide dismutase with a potential role in familial amyotrophic lateral sclerosis (Fujiwara et al. 2007). In the proteasome, cysteine sulfonic acid formation was only identified in the α4 subunit (Schmidt et al. 2006). In the present study, we found that this irreversible modification at the α7 subunit was reduced during apoptosis.

The phosphoproteomic field has advanced significantly during the last few years (Paradela and Albar 2008). However, some sources for false-positive assignments of phosphopeptides based on neutral loss of H_3PO_4 were reported (Lehmann et al. 2007). Here, we found the potassium adduct of an acetylated peptide, which was wrongly assigned as the phosphorylated peptide by the error-tolerant search. However, evaluation of the MS and MS/MS data clarified the real form of the detected peptide.

In conclusion, the analysis of the 20S proteasome during apoptosis showed a quantitative variation of the α7 subunit species α7a and α7b. This speciation has been attributed to posttranslational modifications. Cysteine oxidation has been found in oxidative stress, but was not reported for subunit α7 until now. On the other hand, phosphorylation has been shown to be a key regulatory mechanism to the 20S proteolytic function and might play a role in connection to apoptosis.

Acknowledgments The present study was supported by the National Program for Research in Functional Genomics in Norway (FUGE, project no. 183418/S10) of the Norwegian Research Council to BT.

References

Adrain C, Creagh EM, Cullen SP, Martin SJ (2004) Caspase-dependent inactivation of proteasome function during programmed cell death in *Drosophila* and man. J Biol Chem 279:36923–36930

Alvarez-Castelao B, Castano JG (2005) Mechanism of direct degradation of IkappaBalpha by 20S proteasome. FEBS Lett 579:4797–4802

Arrigo AP, Mehlen P (1993) Hela cells proteasome interacts with leucine-rich polypeptides and contains a phosphorylated subunit. Biochem Biophys Res Commun 194:1387–1393

Bardag-Gorce F, Venkatesh R, Li J, French BA, French SW (2004) Hyperphosphorylation of rat liver proteasome subunits: the effects of ethanol and okadaic acid are compared. Life Sci 75:585–597

Baumeister W, Walz J, Zuhl F, Seemuller E (1998) The proteasome: paradigm of a self-compartmentalizing protease. Cell 92:367–380

Bochtler M, Ditzel L, Groll M, Hartmann C, Huber R (1999) The proteasome. Annu Rev Biophys Biomol Struct 28:295–317

Boelens WC, Croes Y, de Jong WW (2001) Interaction between alphaB-crystallin and the human 20S proteasomal subunit C8/alpha7. Biochim Biophys Acta 1544:311–319

Bose S, Stratford FL, Broadfoot KI, Mason GG, Rivett AJ (2004) Phosphorylation of 20S proteasome alpha subunit C8 (alpha7) stabilizes the 26S proteasome and plays a role in the regulation of proteasome complexes by gamma-interferon. Biochem J 378:177–184

Candiano G, Bruschi M, Musante L, Santucci L, Ghiggeri GM, Carnemolla B, Orecchia P, Zardi L, Righetti PG (2004) Blue silver: a very sensitive colloidal Coomassie G-250 staining for proteome analysis. Electrophoresis 25:1327–1333

Castano JG, Mahillo E, Arizti P, Arribas J (1996) Phosphorylation of C8 and C9 subunits of the multicatalytic proteinase by casein kinase II and identification of the C8 phosphorylation sites by direct mutagenesis. Biochemistry 35:3782–3789

Claverol S, Burlet-Schiltz O, Girbal-Neuhauser E, Gairin JE, Monsarrat B (2002) Mapping and structural dissection of human 20 S proteasome using proteomic approaches. Mol Cell Proteomics 1:567–578

Creasy DM, Cottrell JS (2002) Error tolerant searching of uninterpreted tandem mass spectrometry data. Proteomics 2:1426–1434
Dahlmann B (2005) Proteasomes. Essays Biochem 41:31–48
Dahlmann B, Ruppert T, Kuehn L, Merforth S, Kloetzel PM (2000) Different proteasome subtypes in a single tissue exhibit different enzymatic properties. J Mol Biol 303:643–653
Doherty NS, Littman BH, Reilly K, Swindell AC, Buss JM, Anderson NL (1998) Analysis of changes in acute-phase plasma proteins in an acute inflammatory response and in rheumatoid arthritis using two-dimensional gel electrophoresis. Electrophoresis 19:355–363
Dong J, Chen W, Welford A, Wandinger-Ness A (2004) The proteasome alpha-subunit XAPC7 interacts specifically with Rab7 and late endosomes. J Biol Chem 279:21334–21342
Drews O, Wildgruber R, Zong C, Sukop U, Nissum M, Weber G, Gomes AV, Ping P (2007) Mammalian proteasome subpopulations with distinct molecular compositions and proteolytic activities. Mol Cell Proteomics 6:2021–2031
Froment C, Uttenweiler-Joseph S, Bousquet-Dubouch MP, Matondo M, Borges JP, Esmenjaud C, Lacroix C, Monsarrat B, Burlet-Schiltz O (2005) A quantitative proteomic approach using two-dimensional gel electrophoresis and isotope-coded affinity tag labeling for studying human 20S proteasome heterogeneity. Proteomics 5:2351–2363
Fujiwara N, Nakano M, Kato S, Yoshihara D, Ookawara T, Eguchi H, Taniguchi N, Suzuki K (2007) Oxidative modification to cysteine sulfonic acid of Cys111 in human copper–zinc superoxide dismutase. J Biol Chem 282:35933–35944
Glickman MH, Ciechanover A (2002) The ubiquitin–proteasome proteolytic pathway: destruction for the sake of construction. Physiol Rev 82:373–428
Grubbs FE (1969) Procedures for detecting outlying observations in samples. Technometrics 11:1–21
Guerrero C, Tagwerker C, Kaiser P, Huang L (2006) An integrated mass spectrometry-based proteomic approach: quantitative analysis of tandem affinity-purified in vivo cross-linked protein complexes (QTAX) to decipher the 26 S proteasome-interacting network. Mol Cell Proteomics 5:366–378
Hershko A, Ciechanover A (1998) The ubiquitin system. Annu Rev Biochem 67:425–479
Huang L, Burlingame AL (2005) Comprehensive mass spectrometric analysis of the 20S proteasome complex. Methods Enzymol 405:187–236
Ikeda K, Nakano R, Uraoka M, Nakagawa Y, Koide M, Katsume A, Minamino K, Yamada E, Yamada H, Quertermous T, Matsubara H (2009) Identification of ARIA regulating endothelial apoptosis and angiogenesis by modulating proteasomal degradation of cIAP-1 and cIAP-2. Proc Natl Acad Sci USA 106:8227–8232
Iwafune Y, Kawasaki H, Hirano H (2004) Identification of three phosphorylation sites in the alpha7 subunit of the yeast 20S proteasome in vivo using mass spectrometry. Arch Biochem Biophys 431:9–15
Jin Y, Lee H, Zeng SX, Dai MS, Lu H (2003) MDM2 promotes p21waf1/cip1 proteasomal turnover independently of ubiquitylation. EMBO J 22:6365–6377
Jungblut PR, Seifert R (1990) Analysis by high-resolution two-dimensional electrophoresis of differentiation-dependent alterations in cytosolic protein pattern of HL-60 leukemic cells. J Biochem Biophys Methods 21:47–58
Jungblut PR, Holzhutter HG, Apweiler R, Schluter H (2008) The speciation of the proteome. Chem Cent J 2:16
Keller DM, Zeng X, Wang Y, Zhang QH, Kapoor M, Shu H, Goodman R, Lozano G, Zhao Y, Lu H (2001) A DNA damage-induced p53 serine 392 kinase complex contains CK2, hSpt16, and SSRP1. Mol Cell 7:283–292
Kimura Y, Takaoka M, Tanaka S, Sassa H, Tanaka K, Polevoda B, Sherman F, Hirano H (2000) *N*(alpha)-acetylation and proteolytic activity of the yeast 20 S proteasome. J Biol Chem 275:4635–4639
Koehler CJ, Strozynski M, Kozielski F, Treumann A, Thiede B (2009) Isobaric peptide termini labeling for MS/MS-based quantitative proteomics. J Proteome Res 8:4333–4341
Kuckelkorn U, Ruppert T, Strehl B, Jungblut PR, Zimny-Arndt U, Lamer S, Prinz I, Drung I, Kloetzel PM, Kaufmann SH, Steinhoff U (2002) Link between organ-specific antigen processing by 20S proteasomes and CD8(+) T cell-mediated autoimmunity. J Exp Med 195:983–990
Laemmli UK (1970) Cleavage of structural proteins during the assembly of the head of bacteriophage T4. Nature 227:680–685
Lehmann WD, Kruger R, Salek M, Hung CW, Wolschin F, Weckwerth W (2007) Neutral loss-based phosphopeptide recognition: a collection of caveats. J Proteome Res 6:2866–2873
Lim JC, Choi HI, Park YS, Nam HW, Woo HA, Kwon KS, Kim YS, Rhee SG, Kim K, Chae HZ (2008) Irreversible oxidation of the active-site cysteine of peroxiredoxin to cysteine sulfonic acid for enhanced molecular chaperone activity. J Biol Chem 283:28873–28880
Ling MT, Chiu YT, Lee TK, Leung SC, Fung MK, Wang X, Wong KF, Wong YC (2008) Id-1 induces proteasome-dependent degradation of the HBX protein. J Mol Biol 382:34–43
Liu CH, Goldberg AL, Qiu XB (2007) New insights into the role of the ubiquitin–proteasome pathway in the regulation of apoptosis. Chang Gung Med J 30:469–479
Lu H, Zong C, Wang Y, Young GW, Deng N, Souda P, Li X, Whitelegge J, Drews O, Yang PY, Ping P (2008) Revealing the dynamics of the 20 S proteasome phosphoproteome: a combined CID and electron transfer dissociation approach. Mol Cell Proteomics 7:2073–2089
Ludemann R, Lerea KM, Etlinger JD (1993) Copurification of casein kinase II with 20 S proteasomes and phosphorylation of a 30-kDa proteasome subunit. J Biol Chem 268:17413–17417
Mason GG, Hendil KB, Rivett AJ (1996) Phosphorylation of proteasomes in mammalian cells. Identification of two phosphorylated subunits and the effect of phosphorylation on activity. Eur J Biochem 238:453–462
Mittenberg AG, Moiseeva TN, Barlev NA (2008) Role of proteasomes in transcription and their regulation by covalent modifications. Front Biosci 13:7184–7192
Olsen JV, de Godoy LM, Li G, Macek B, Mortensen P, Pesch R, Makarov A, Lange O, Horning S, Mann M (2005) Parts per million mass accuracy on an Orbitrap mass spectrometer via lock mass injection into a C-trap. Mol Cell Proteomics 4:2010–2021
Ong SE, Blagoev B, Kratchmarova I, Kristensen DB, Steen H, Pandey A, Mann M (2002) Stable isotope labeling by amino acids in cell culture, SILAC, as a simple and accurate approach to expression proteomics. Mol Cell Proteomics 1:376–386
Orlowski RZ, Kuhn DJ (2008) Proteasome inhibitors in cancer therapy: lessons from the first decade. Clin Cancer Res 14:1649–1657
Orlowski M, Wilk S (2003) Ubiquitin-independent proteolytic functions of the proteasome. Arch Biochem Biophys 415:1–5
Paradela A, Albar JP (2008) Advances in the analysis of protein phosphorylation. J Proteome Res 7:1809–1818
Pardo PS, Murray PF, Walz K, Franco L, Passeron S (1998) In vivo and in vitro phosphorylation of the alpha 7/PRS1 subunit of *Saccharomyces cerevisiae* 20 S proteasome: in vitro phosphorylation by protein kinase CK2 is absolutely dependent on polylysine. Arch Biochem Biophys 349:397–401
Perkins DN, Pappin DJ, Creasy DM, Cottrell JS (1999) Probability-based protein identification by searching sequence databases using mass spectrometry data. Electrophoresis 20:3551–3567
Rabl J, Smith DM, Yu Y, Chang SC, Goldberg AL, Cheng Y (2008) Mechanism of gate opening in the 20S proteasome by the proteasomal ATPases. Mol Cell 30:360–368

Raijmakers R, Berkers CR, de Jong A, Ovaa H, Heck AJ, Mohammed S (2008) Automated online sequential isotope labeling for protein quantitation applied to proteasome tissue-specific diversity. Mol Cell Proteomics 7:1755–1762

Rechsteiner M, Hill CP (2005) Mobilizing the proteolytic machine: cell biological roles of proteasome activators and inhibitors. Trends Cell Biol 15:27–33

Rivett AJ, Mason GG, Thomson S, Pike AM, Savory PJ, Murray RZ (1995) Catalytic components of proteasomes and the regulation of proteinase activity. Mol Biol Rep 21:35–41

Schluter H, Apweiler R, Holzhutter HG, Jungblut PR (2009) Finding one's way in proteomics: a protein species nomenclature. Chem Cent J 3:11

Schmidt F, Dahlmann B, Janek K, Kloss A, Wacker M, Ackermann R, Thiede B, Jungblut PR (2006) Comprehensive quantitative proteome analysis of 20S proteasome subtypes from rat liver by isotope coded affinity tag and 2-D gel-based approaches. Proteomics 6:4622–4632

Schmidt F, Strozynski M, Salus SS, Nilsen H, Thiede B (2007) Rapid determination of amino acid incorporation by stable isotope labeling with amino acids in cell culture (SILAC). Rapid Commun Mass Spectrom 21:3919–3926

Schmidt F, Fiege T, Hustoft HK, Kneist S, Thiede B (2009) Shotgun mass mapping of *Lactobacillus* species and subspecies from caries related isolates by MALDI-MS. Proteomics 9:1994–2003

Sdek P, Ying H, Chang DL, Qiu W, Zheng H, Touitou R, Allday MJ, Xiao ZX (2005) MDM2 promotes proteasome-dependent ubiquitin-independent degradation of retinoblastoma protein. Mol Cell 20:699–708

Shu F, Guo S, Dang Y, Qi M, Zhou G, Guo Z, Zhang Y, Wu C, Zhao S, Yu L (2003) Human aurora-B binds to a proteasome alpha-subunit HC8 and undergoes degradation in a proteasome-dependent manner. Mol Cell Biochem 254:157–162

Sun XM, Butterworth M, MacFarlane M, Dubiel W, Ciechanover A, Cohen GM (2004) Caspase activation inhibits proteasome function during apoptosis. Mol Cell 14:81–93

Tanaka K, Tanahashi N, Tsurumi C, Yokota KY, Shimbara N (1997) Proteasomes and antigen processing. Adv Immunol 64:1–38

Thiede B, Hohenwarter W, Krah A, Mattow J, Schmid M, Schmidt F, Jungblut PR (2005) Peptide mass fingerprinting. Methods 35:237–247

Touitou R, Richardson J, Bose S, Nakanishi M, Rivett J, Allday MJ (2001) A degradation signal located in the C-terminus of p21WAF1/CIP1 is a binding site for the C8 alpha-subunit of the 20S proteasome. EMBO J 20:2367–2375

Tsimokha AS, Mittenberg AG, Kulichkova VA, Kozhukharova IV, Gause LN, Konstantinova IM (2007) Changes in composition and activities of 26S proteasomes under the action of doxorubicin-apoptosis inductor of erythroleukemic K562 cells. Cell Biol Int 31:338–348

Uttenweiler-Joseph S, Claverol S, Sylvius L, Bousquet-Dubouch MP, Burlet-Schiltz O, Monsarrat B (2008) Toward a full characterization of the human 20S proteasome subunits and their isoforms by a combination of proteomic approaches. Methods Mol Biol 484:111–130

Wang X, Chen CF, Baker PR, Chen PL, Kaiser P, Huang L (2007) Mass spectrometric characterization of the affinity-purified human 26S proteasome complex. Biochemistry 46:3553–3565

Wehren A, Meyer HE, Sobek A, Kloetzel PM, Dahlmann B (1996) Phosphoamino acids in proteasome subunits. Biol Chem 377:497–503

Yi P, Feng Q, Amazit L, Lonard DM, Tsai SY, Tsai MJ, O'Malley BW (2008) Atypical protein kinase C regulates dual pathways for degradation of the oncogenic coactivator SRC-3/AIB1. Mol Cell 29:465–476

Ying J, Clavreul N, Sethuraman M, Adachi T, Cohen RA (2007) Thiol oxidation in signaling and response to stress: detection and quantification of physiological and pathophysiological thiol modifications. Free Radic Biol Med 43:1099–1108

Zhang Z, Torii N, Furusaka A, Malayaman N, Hu Z, Liang TJ (2000) Structural and functional characterization of interaction between hepatitis B virus X protein and the proteasome complex. J Biol Chem 275:15157–15165

Zimny-Arndt U, Schmid M, Ackermann R, Jungblut PR (2009) Classical proteomics: two-dimensional electrophoresis/MALDI mass spectrometry. Methods Mol Biol 492:65–91

Zong C, Young GW, Wang Y, Lu H, Deng N, Drews O, Ping P (2008) Two-dimensional electrophoresis-based characterization of post-translational modifications of mammalian 20S proteasome complexes. Proteomics 8:5025–5037